Designing a COTS electronic system for trajectory correction of a Radio controlled model electrical car

DONDON (1)- A.DUTREY (2)- J.B BOURLIER (2)- A. SIVERT (3)
(1) Université de Bordeaux, IPB Av Dr A. Schweitzer 33405 Talence, НТСР EG
(2) Université de Bordeaux IUT GEII, 15 rue Naudet 33175 GRADIGNAN
(3) Institut Universitaire de Technologie, Laboratory for Innovative Technologies (L.T.I), Team
Energy Electric and Associated System – SOISSONS, НТСР EG
Philippe.Dondon@enseirb-matmeca.fr, arnaud.sivert@u-picardie.fr

Abstract: The study relates to the design and the realization of an electronic trajectory stabilisation system for a RC (Radio Controlled) model electrical car. We give first the context of the study and the mains specifications. Available hardware (mechanical parts, sensors) are briefly described. Then, characterisation and modelling of the steering wheels control system is proposed. The electronic design and software implementation are exposed and we show some experimental results and validation tests. The trajectory correction strategy is secondly explained; used sensors are described and characterized. Finally, a feed back electronic system is proposed before comments and technical discussion.

Key words: MEMS sensor, Power control, Analogue electronic, Electronic feed back, R/C electrical model car, Multi thematic project, Pedagogical experience.

1 Introduction

1.1 ENSEIRB MATMECA, a graduate engineering school

The "Ecole Nationale Supérieure d'Electronique, Informatique et Radiocommunications de Bordeaux" (ENSEIRB) is one of the national graduate engineering schools, known as 'Grandes Ecoles' in France. It was founded in 1920. Even though it is an independent structure, ENSEIRB is closely linked to the Bordeaux 1 Science and Technology University. ENSEIRB has developed with the growth of information and communication technologies. A Computer Science Department was created in 1986 to complement the original Electronics Department. The expansion has proceeded in year 2000, with the development of a new Department of Telecommunications.

1.2 Laboratory collaboration

The study presented here, was carried out at the IPB/ ENSEIRB MATMECA in collaboration with Laboratory for Innovative Technologies of Soissons.

2 The project context

2.1 General safety aspects of vehicle motion

Around one car accident on four is due to a slip outside of the road. According to the international surveys, 30 to 50% of the fatal route exits would be prevented if the car were equipped with one ESP. Following the example ABS (anti-locking braking), ESP (control of stability) [1] is an electronic help with the conduit of paramount importance. ABS [2] avoids the wheel locking during a braking phase, which makes it possible the vehicle to remain right. ESP, as for him, slows down certain wheels in the event of skid individually, in order to stabilize the vehicle. The two systems need sensors [3], [4] in particular for measuring the angular speed [5], [6] of the wheels and the side acceleration of the car.

2.2 ENSEIRB-MATMECA context

Since a few years, some ENSEIRB MATMECA students show an increasing interest for vehicles embedded electronics system. In particular, the well

known ESP/ABS control system looks quite "mysterious" for many people and causes many questions.

So, as it is almost impossible to perform tests on real size vehicle for pedagogical, financial and safety reasons, we decided to start the design of a similar but of course simplified electronic system for a small scale model RC electrical car.

Even if the complexity of our system is far from the reality, [7] it is enough for the students to understand the principles of the ESP system and to get a right idea of what we can do with sophisticated sensors such as accelerometer and gyroscope.

2.3 Learning by project at ENSEIRB MATMECA

The project we present here, takes place in the "learning by project" strategy in our scientific school which is quite recent (around eight years). The aim of this approach [8], [9] is to optimize the motivation and to develop the curiosity of the students by a practical approach and a "bottom up" teaching strategy.

3 Description of the project

3.1 General description

3.1.1 Aim of the project

The aim of this project is to design an electronic system with an embedded software to drive as simply as possible an autonomous RC (radio controlled) small model electric car: In case of side displacement (lateral wind or shock) of the car, or back skid (wet or frozen floor), the system must compensate by itself, by "against directing" the front wheels. For "easy design" reasons, correction is applied only on steering wheels and we do not manage propulsion power. For safety reasons a front obstacle detector must be mounted on the nose of the car.

3.1.2 Main characteristics of the small model car.

For this purpose, we use a mechanical 1/14 sclae frame from Nikko Company [10] as indicated in figure 1a and 1b.

The main characteristics of this model are:

- Remote control: AM 26MHz, two channels PWM
- 1/14 scale, Length: 320mm, Width: 170mm,
- Weight: # 640g depending on equipment
- Suspension: 4 independent wheels,
- Propulsion Engine: Mabuchi RC-280SA DC permanent magnet motor 9,6V 4A,
- Maximum speed =20km/h (i.e. 5,5m/s)
- Body Type: Polycarbonate Cut & Printed
- Differential rear gear system
- Tyre Width: Front 20mm, Rear 25mm
- Tyre Diameter: 48mm. (smooth-tread tyres)
- Steering wheels control: Mabuchi RF-020TH DC motor + 5kΩ rotative potentiometer position sensor.
- Minimum turning radius : 35cm

Figure 1a: Small scale Peugeot 206 WRC Nikko (1/14)

Figure 1b: Body of small scale model car

For our project, we removed the Nikko electronic circuits. We kept only the mechanical frame, in order to install our own electronic boards.

3.2 Technical specifications

The main electronic specifications for the project are:

- Power supply: 9,6V 6500mAh NiCd battery cell
- Microcontroller board: classical MICROCHIP controller 16F876 (to be designed)
- Electronic MEMS accelerometers from Freescale
- Traction motor control (to be designed)
- Steering wheels control: (to be designed)
- Infrared detection of a front obstacle from Sharp

3.3 Quick hardware description

3.3.3 Steering motor [11]

The front wheels of the vehicle are moved by a Mabushi DC motor RF-020TH (figure 2) and a gear box. It is connected to a mechanical toothed rack and rod of direction. The angular position is given by a rotating potentiometer coupled to the gears.

Figure 2: Mabushi steering motor
(Diameter 17,7mm, length 24mm, weight 16gr)

The figure 3 shows the basic electronic driver of the steering motor.
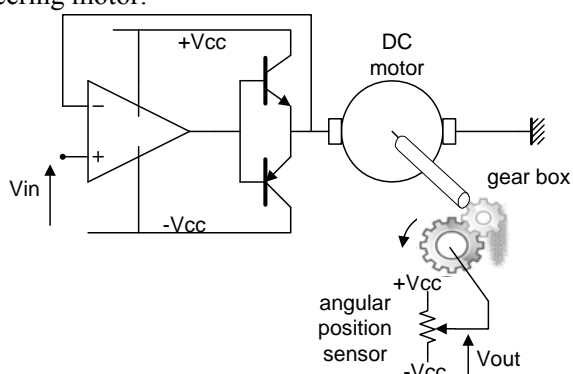
Figure 3: Steering motor driver

Power consumption of the servo during rotation is around 150mA depending, of course, of the friction resistant couple (cf. behaviour characterisation in § 4.1 and modelling in § 5.1).

The electronic design of the angular position feed back control is detailed in § 6.3.

3.3.5 Propulsion engine

The Mabuchi DC motor RC-280SA, [12] located close to the rear wheels, will be driven by a full H bridge and a PWM signal to control the speed. (see design details in § 5.2).

3.3.6 Infrared Front sensors

For safety reasons, a front obstacle detection has been implemented using a classical SHARP GP2D15 (Figure 6) Infrared sensor [8] as on/off detection up to 80 cm. The advantage of this type of sensor is that it is not sensible to the reflectance properties of the obstacle.
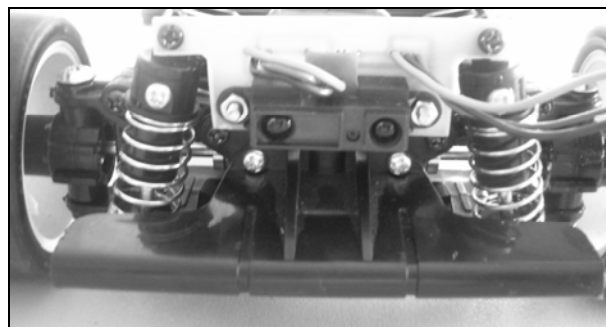

Figure 4: Infrared sensor Sharp GP2D15

The threshold detection distance is set up to 40 cm, which is sufficient to slow down the car and to avoid a brutal shock.

4 System characterisation

Most of the detailed electronic and mechanical performances of the small model car are unfortunately, unknown like often in the "RC hobbyist world". So, we explain in the paragraph, how we extract the main characteristics through experimentation.

4.1 Steering servo motor characterisation

As we don't have the electronic and mechanical specifications of the steering motor, we first identify its behaviour by analyzing the pulse response:

This test has been performed under normal operating conditions, i.e. including mechanical backlash and ground-wheel frictions.
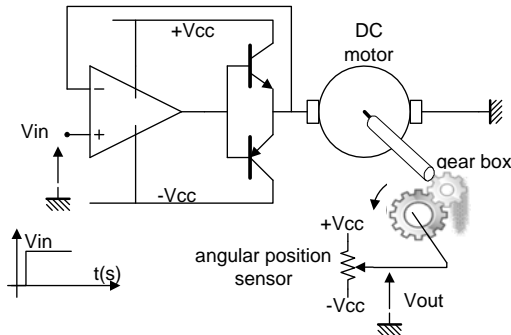

Figure 5: steering motor test board

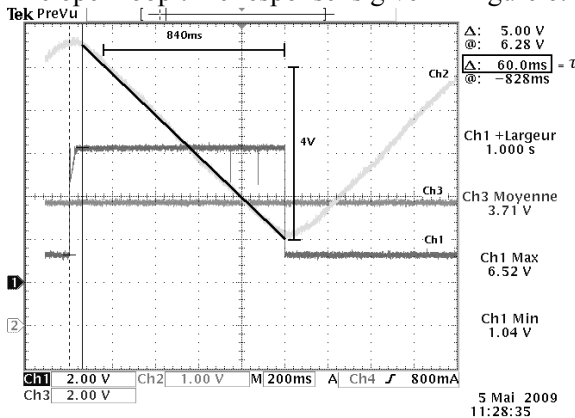The open loop time response is given in figure 6.

Figure 6: unit pulse response (Vout vs Vin)
Trace 1 : Vin, 2V/div
Trace 2 : Vout, 2V/div Horizontal scale: 200ms/div

We observe a constant time delay and then a linear slope. Extracted modelling parameters are given in §.5.1

4.2 Small car movement first characterisation
The aim of the characterisation is to obtain a modelling as simple as possible which represents the mechanical behaviour of the assembly.
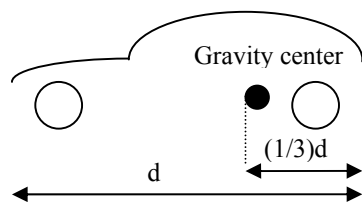

Figure 7: Gravity center location

Our car is naturally "over steer" because the center of gravity is located close to the rear wheels (cf. figure 7). Moreover, the rear propulsion facilitates the back slip. At least, the extremely low location of the gravity center always ensures a slip before a swing of the vehicle. For a first approach, we thus chose to use the elementary laws of object movement to characterize our car.
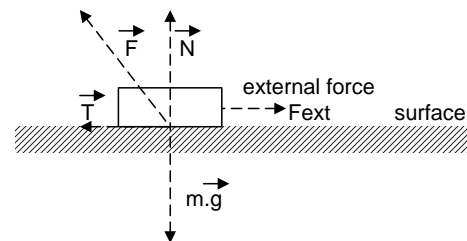

Figure 8: General friction force diagram

Figure 8 shows the forces applied on a solid by considering the weight (m. $\vec{g}$), normal reaction of the floor surface $\vec{N}$, dry frictions $\vec{T}$, and external force $\vec{F}_{ext}$ (traction). From the Amonton and Coulomb law's, we know that the necessary threshold force $\vec{T}$ to start the movement do not depend on the contact area but it is proportional to the normal reaction $\vec{N}$: The proportionality coefficient changes depending on the materials nature.
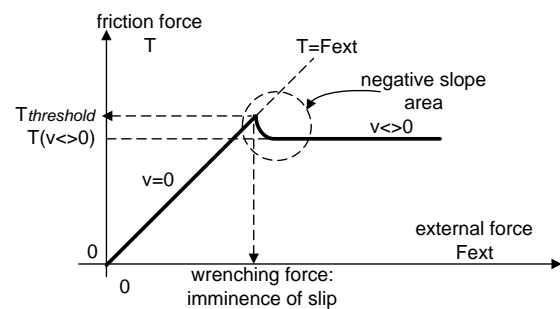

Figure 9: Threshold slip force level

We define μs the static friction coefficient:

$$\frac{T_{threshold}}{N} = \mu_s$$

Moreover, if there is slip, the friction force T(v<>0) does not depend on speed. And we get the kinetic friction coefficient μc:

$$\frac{T_{(v \neq 0)}}{N} = \mu_c$$

At least, the zone with negative slope on figure 9 can be compared in electronics to a zone of "negative resistance" and thus to a zone of instability (alternation of slip and resumption of adherence as a piece of chalk which grates on a blackboard). This part of the curve is difficult to finely model.

The table 1 hereafter, gives the coefficients of friction for some usual materials.

Classical body to body friction	μs	μc
Stain/Stain smooth surface	100	100
Wood /Wood	0.5	0.3
Metal/Ice	0.03	0.01
Tyres/ Dry road	0.8	0.6
Tyres/ Wet road	0.15	0.1

Table 1: Static and kinetics friction coefficients for some classical materials.

In our case, one can evaluate these coefficients of friction knowing the weight of our small scale model car, with the experimentation given in figure 10, depending on different nature of the floor.
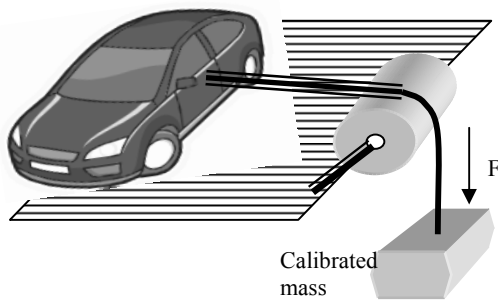

Figure 10: Friction force and coefficients experimental determination

We carried out several tests on grounds of different nature. And we made a useful comparison with the coefficients given in table 2, to validate the experiment. In the same experiment, we obtain a pratical value of $T_{threshoLd}$ on a given floor for a lateral slipping :

$T_{threshoLd} = 4, 41$ Newton on smooth floor
$T_{threshoLd} = 10$ Newton on rough floor

All these characterisations were useful for the slipping behaviour understanding, and are used in the paper "part two".

Small model car tyres friction	μs	μc
Rubber tyres /smooth floor (dry)	0.66	0.42
Rubber tyres /smooth floor (wet)	0.1	0.05
Rubber tyres / rough surface (dry)	10	10
Rubber tyres / rough surface (wet)	6	7

Table 2: Friction coefficients of our model car

5 R/C small car modelling

5.1 Steering motor modelling

From characterisation exposed in § 4.2, and figure 6, we extract the main time constant of the steering motor. And we obtain a simplified modelling as indicated in figure 12, where K = 10 and τ = 100ms.

A quick ABM (Analogue Behaviour Modelling) in Spice Simulator, allowed us to check our modelling validity and fitting (cf. figure 13).
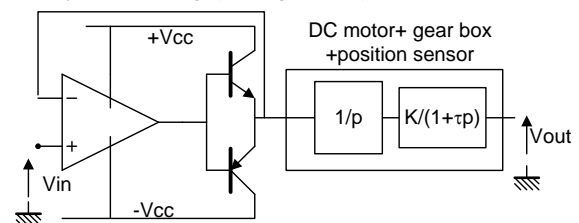

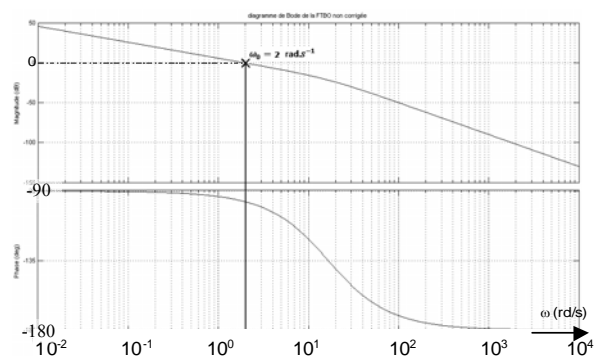Figure 12: Steering motor modelling

Figure 13: Corresponding open loop frequency response gain in dB (upper trace, 50dB/div) and phase in ° (lower trace, 45°/div)

This preliminary modelling allows a correct electronic design of the position feed back loop and P.I.D correction (cf. § 6.1)

5.2 Propulsion modelling

The aim of this paragraph is to get a representation of the propulsion behaviour and driving conditions which generates a possible slip in curve. It will help the R/C car pilot to improve the understanding of the small model car and to have a finer control of Remote Control emitter joystick position.

Propulsion of the car is done by a Mabuchi DC motor RC-280SA, located close to the rear wheels. It is driven by a full H bridge and a PWM signal to control the speed.

5.2.1 PWM duty cycle limit determination

At first order, the car speed v is proportional to the PWM signal duty cycle α as indicated on figure 14a (obtained from indoor test).
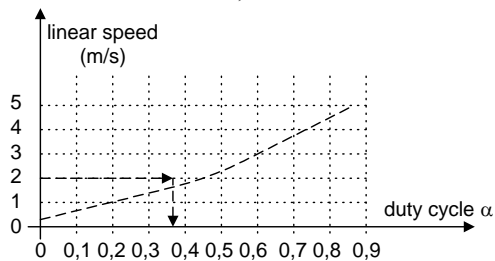

Figure 14a: linear speed vs. PWM duty cycle

For a given floor, we can determine a limit value of the PWM duty cycle signal which generates a slipping risk during a curve as follow:

From paragraph §4.2, $T_{threshold} = mv_l^2/R$ where "m" is mass of the vehicle and R the curve radius.

Then, we estimate the maximum tangential speed in curve $Vl = \sqrt{\dfrac{T_{threshold}.R}{m}} = \sqrt{\mu s.g.R}$ before slipping, as a function of curve radius.
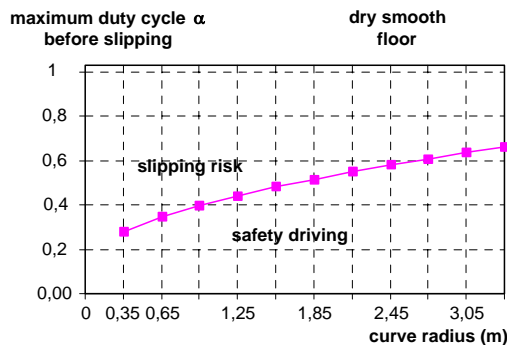

Figure 14b: max duty cycle α, starting the slip vs curve radius R

Knowing the supply voltage, µs and from figure 14a, v=f(α), we can obtain the curve figure 14b: maximum duty cycle vs. curve radius for a dry floor (on the example) which start up the slip.

6 Electronic design

6.1 General synoptic

The whole schematic diagram of the R/C car embedded electronic is given in figure 15.
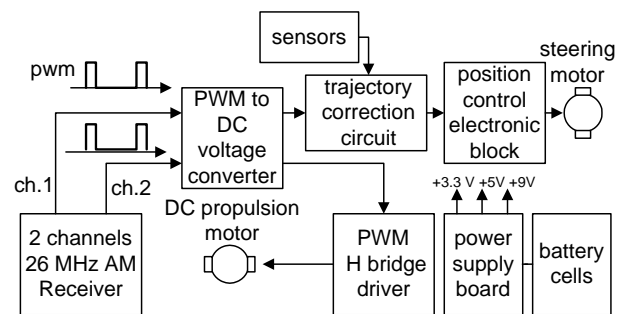

Figure 15: General block diagram

The AM receiver delivers 2 PWM signals 50Hz, 1 to 2 ms pulse width, corresponding to the RC joystick movements, according to Radio Control systems standards. Chanel 1 is used to control the steering motor (see §6.3) while channel 2 drives the propulsion engine through our electronic modules. The PWM to DC voltage converter converts the received PWM signal in proportional analogue set up voltage.

All the modules were designed during the project except the commercial AM receiver. Trajectory correction theory, accelerometers uses and processing circuit design are detailed in paper "part two".

6.2 PWM to DC voltage converter design

The PWM to DC voltage converter converts the two received PWM signals, in proportional analogue set up voltage for feed back loop ESP processing. For this design we used a classical PIC 16F876 controller programmed in C language and two AD 558 D/A converter.

6.3 Steering servo position control system design

This block has been designed with full analogue components: it consists of one gain comparator stage, PID corrector, push pull stage and battery middle point circuit as shown in figure 21.
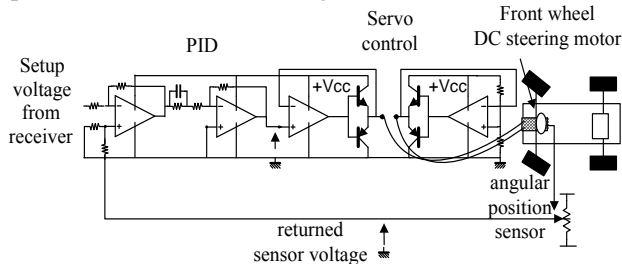

Figure 21: Steering servo motor control

The PID effect and closed loop response of the system after PID correction were checked with Matlab software.
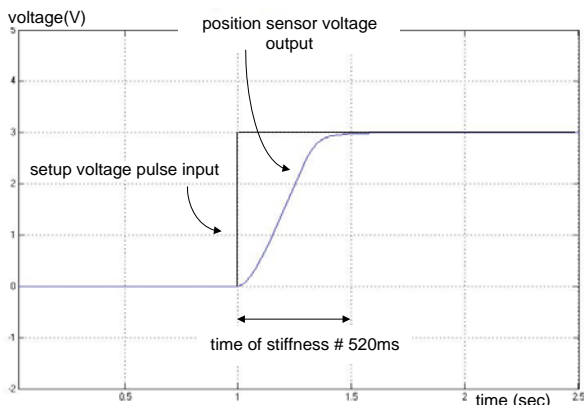

Figure 22: Closed loop response (MATLAB simulation)

6.4 Traction DC Motor and PWM driver

In order to simplify the design, we uses a basic H full bridge switching structure circuit L298 sized for a maximum current of 4 Amps [13]. 0 to 100% PWM signal is generated at 18 kHz to avoid audible noise. An input on the logical gate allows stopping the car in case of emergency or front obstacle detection during the motion.

Enable and direction signals (move forward or backwards) are generated by the microcontroller.

6.5 Full equipped small scale model car

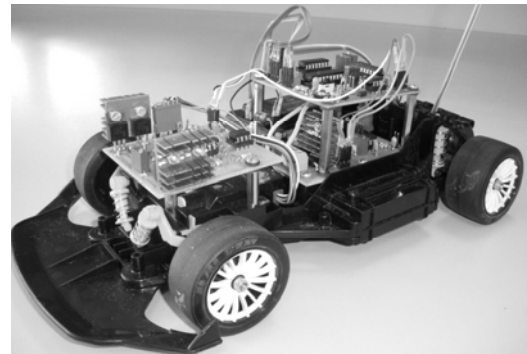The full equipped car is shown in figure 23.

Figure 23: model car opened

When the car is in action, the motor generates some electromagnetic perturbations, so that we added a copper shield and we put the electronic module as far as possible from the DC motor.

7 Validation tests

7.1 Electrical test

The figure 24 shows typical waveform (according to the H bridge theory) we obtain with this propulsion motor driver.
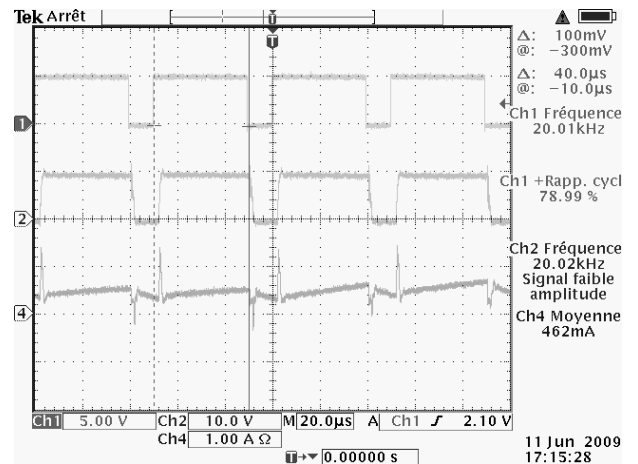

Figure 24: experimental voltage and current waveforms through the propulsion motor

Trace 1: logical control PWM signal 5V/div
Trace 2: voltage across the propulsion motor
Trace 4: Current through the motor (scale: 1A/div)
(forward propulsion = positive current and backward propulsion = negative current)

The figure 25 shows the closed loop response of steering motor to a setup voltage pulse (corresponding to the schematic figure 21). We check a good matching between simulation (cf. figure 22) and experimental behaviour, time of stiffness as predicted.)
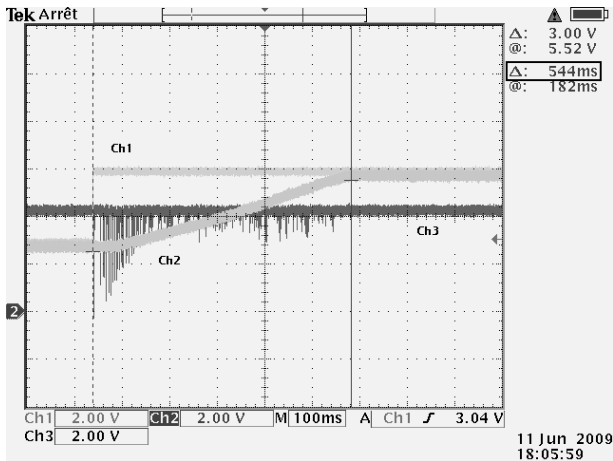

Figure 25: steering motor pulse closed loop response

Trace 1: input setup voltage pulse (corresponding full rotation of the front wheel to the right) 2V/div
Trace 2: position sensor output voltage 2V/div

8 Trajectory modelling

8.1 Introduction
Some modelling (Bicycle, Ackerman) exists to model the behaviour in curve trajectory [14,15]. These modelling led to a complete behaviour modelling including mathematical and non linear aspects too much complex for our first approach.
Thus, we chose a simplified and more practical approach by neglecting second order effects such as non linear tyres deformation. We also assume that the motion of the R/C car is stationary and circular during the curves. A geometrical approach is then possible as described in the next paragraph.

8.2 Hypothesis
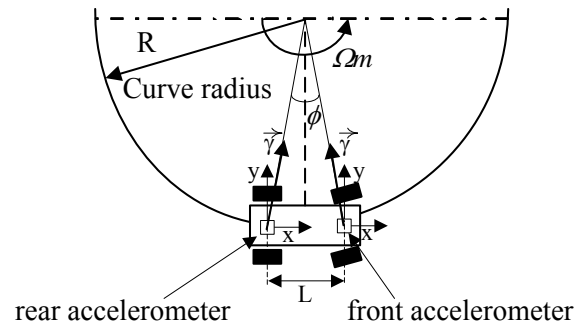The idea is to place two accelerometers [4], [6, [15] (two axis x, y) as indicated in figure 3.

Figure 3: small model car in curve

Let the mains variables to be:
L : distance between accelerometers,
R : curve radius (L=R.ϕ),
V : tangential speed = linear speed when entering in the curve, (V=R. Ω_m) with Ω_m angular speed,
$|\gamma|$: centripetal acceleration $|\gamma|$= v^2/R= Ω^2_m.R

8.3 Normal turn (without slip)
Acceleration vector projection on « y » axis are identical
$\gamma_y = |\gamma|.\cos (\phi/2)$
Acceleration vector projection on « x » axis are identical in module but opposite sign.

8.4 Slipping turn

Assuming that:
θ = is the slipping angle referenced to the normal vector (Cf. figure 4)
We have on the front accelerometer:
$|\gamma_f|.=\Omega^2_m.R$ $\quad\quad\quad\quad\quad$ (1)

And the "x" and "y" two axis projections:
$\gamma_{fx} = |\gamma_f|.\cos \theta$
$\gamma_{fy} = |\gamma_f|.\sin \theta$
Finally:
$\gamma_{fx} = \Omega^2_m.R.\cos \theta$ $\quad\quad\quad\quad$ (2)
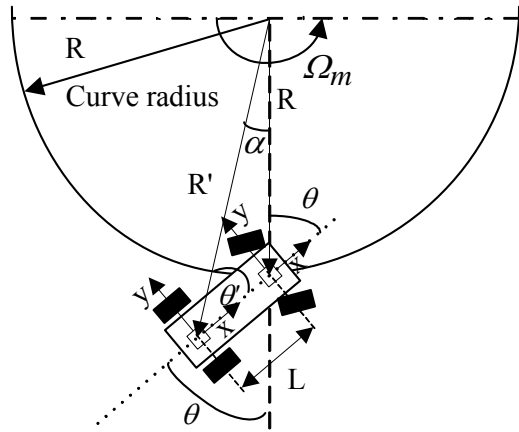$\gamma_{fy} = \Omega^2_m.R.\sin \theta$ $\quad\quad\quad\quad$ (3)

Figure 4: slipping during curve

On the rear accelerometer:

$$|\gamma_r| = \Omega^2_m.R' \qquad (4)$$

Where :

$$R' = \sqrt{R^2 + L^2 + 2.R.L\cos\theta} \qquad (5)$$

And the two axis acceleration vector projections:

$$\gamma_{rx} = |\gamma_r|.\cos\theta' \qquad (6)$$
$$\gamma_{ry} = |\gamma_r|.\sin\theta' \qquad (7)$$

By geometrical considerations :

$$\theta' + \alpha + (\pi - \theta) = \pi$$

Thus : $\theta' = \theta - \alpha$

And :
$$R'.\sin\alpha = L.\sin\theta$$

It yields :

$$\alpha = \arcsin\left[(L/\sqrt{R^2 + L^2 + 2.R.L\cos\theta}).\sin\theta\right]$$

And finally :

$$\gamma_{rx} = (\Omega^2_m . \sqrt{R^2 + L^2 + 2.R.L\cos\theta}).\cos\theta' \qquad (8)$$
$$\gamma_{ry} = (\Omega^2_m . \sqrt{R^2 + L^2 + 2.R.L\cos\theta}).\sin\theta' \qquad (9)$$

With :

$$\theta' = \theta - \arcsin\left[(L/\sqrt{R^2 + L^2 + 2.R.L\cos\theta}).\sin\theta\right]$$

8.5 Possible exploitations of sensor's datas
The difference between the two accelerometers on x is:

$$\Delta\gamma_x = \gamma_{fx} - \gamma_{rx} = |\gamma_r|.\cos\theta' - |\gamma_f|.\cos\theta$$

That is:

$$\Omega^2_m.(\sqrt{(R^2 + L^2 + 2.R.L\cos\theta)}.\cos\theta' - R.\cos\theta) \qquad (10)$$

One can show by tabulation computation of this expression, normalized to the angular velocity, the value is constant: $\Delta\gamma x/\Omega^2_m = 1$. With a similar approach we obtain: $\Delta\gamma y/\Omega^2_m = 0$ whatever the θ angle. We can quote that changes in $\Delta\gamma_x$ will only occur during transient phase "no slipping->slipping start. We speak then about variation of acceleration which is known as "jerk" $(\delta\gamma/\delta t)$.

Thus, in a stabilized slipping situation, the difference value is not exploitable for slipping detection state.

In an other hand, the ratio $|\gamma_r|/|\gamma_f|$ and the product of x axis $\gamma_{fx}.\gamma_{rx}$ projections (Normalized to Ω^2_m.) are depending of θ angle (cf. figure 5).

Figure 5 -obtained from Excel Microsoft tabulated equation (1) to (10)- show the different possible exploitation of sensor's data: x projection difference, x projection multiplication, modules multiplication, as a function of slipping angle θ normalized to Ω^2_m, with L=10cm and minimum curve radius R= 35cm.

The multiplication of x axis acceleration vector projections gives the best sensitivity and a quasi proportionality with the slipping angle: ratio max/min value of 10 for θ varying from 0 to 90°, against a ratio of 2 for the module ratio, and small ratio of 1.2 for the module multiplication. This information is then suitable for a proportional against steering.
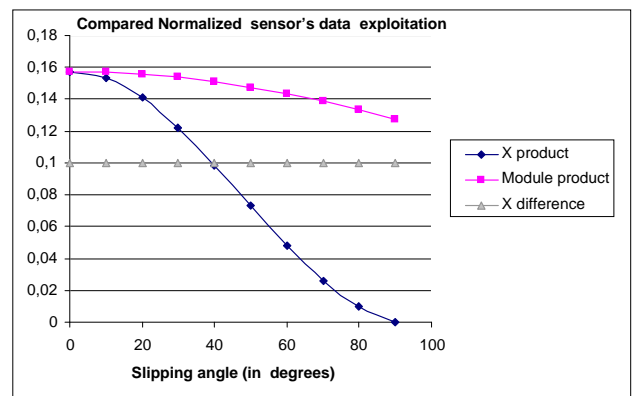

Figure 5: Comparison of sensor processing strategies

8.6 Slipping detection

From the previous paragraph § 4.5, the computation of x projection value and jerk detection allow to get information on slipping beginning and width.

For the first electronic design, we will use only $\Delta\gamma_x$ variation that is "jerk" detection.

Sign or direction of slipping will be obtained thank to a gyro module [17] which is easily able to measure the curve direction. And we will make an action only on steering wheels.

9. MEMS Accel erometer description and characterisation

9.1 Three axis accelerometer module description

Figure 6: Accelerometer module "MMA7260Q" Freescale inc

We use accelerometers to measure two axis lateral and axial acceleration [15,16,17].

This MEMS circuit uses switched capacitor techniques to measure the g-cell capacitors and extract the acceleration data from the difference between the two capacitors.

The main characteristics are given in table 1.

Parameters	Symbol	Specification			Unit
		Min/Typical/Max			
Supply	V_{CC}	2.2	3.3	3.6	V
Full scale	gfs	±1.5g	-	±6g	m/s2

Table 1: MMA7260Q technical characteristics

9.2 Accelerometer test bench

We first checked the sensitivity and reaction of the accelerometers module by placing it on a hand made rotating turret (cf. figure 7) to simulate the car in rotation. We measured the sensitivity value, linearity, saturation time constant due to internal filters, and electronic conditioning circuits characteristics. From this characteristation we stated the design as indicated in paragraph § 6.
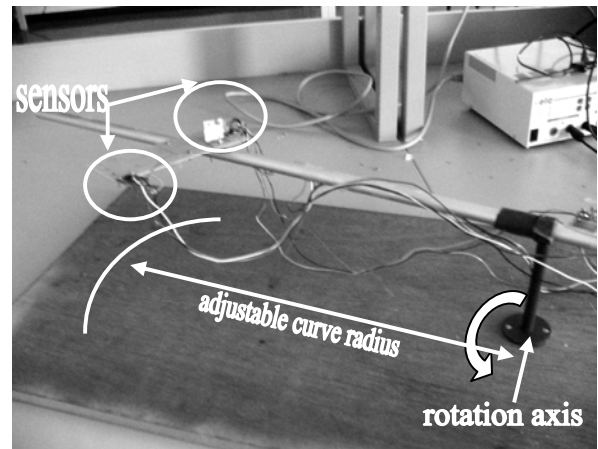
Figure 7: Accelerometer test bench

10. Feed back loop electronic design

10.1 Sensor processing circuit design

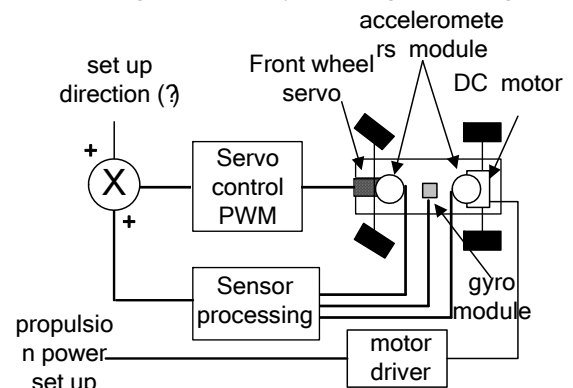The block diagram of the system is given in figure 8.

Figure 8: Feed back loop diagram

The detailed sensor block diagram is shown in figure 9. Electronic design is based on COTS analogue components and classical functions such amplification, L.P filters (to reject mechanical vibrations), comparison…

For this first design, a fixed voltage correction is generated for a full against steering. (See paragraph 8.3 for possible improvement).
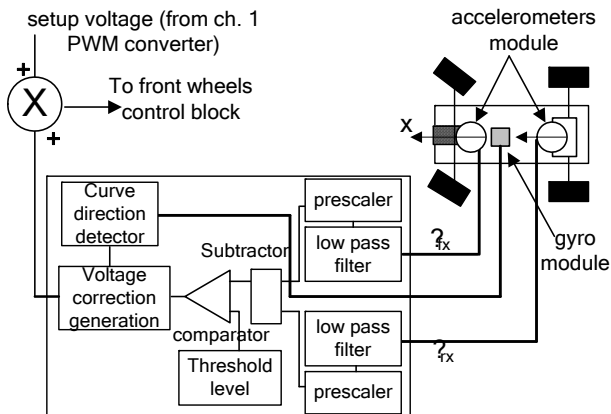
Figure 9: sensor processing internal diagram

11. Final validation tests

11.1 Electrical test

The figure 11 shows the response of accelerometers, when a sudden slipping appears during curve. (jerk detection).

Figure 11: Jerk detection

Ch 1:   X output rear and front accelerometer difference (vert. scale: 200mV/div)
Ch 2: positive input of hyteresis comparator (vert. scale: 200mV/div)
Ch 3 : output voltage, jerk detection (vert. Scale: 5V/div).

Figure 12 shows the signals from gyroscope for curve direction detection.
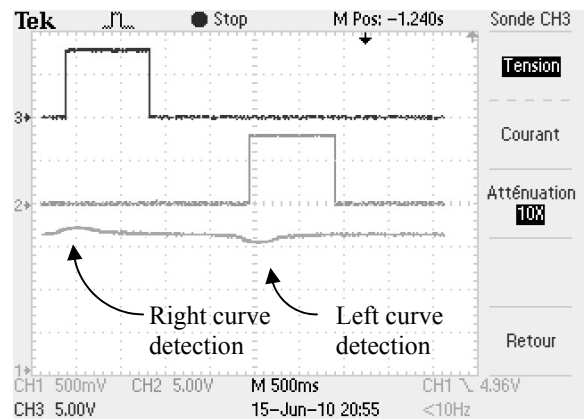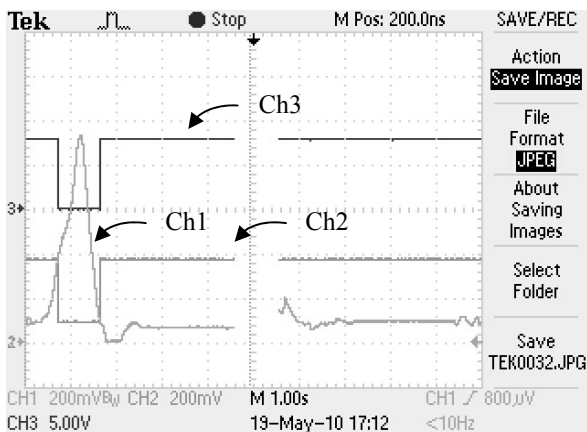

Figure 12 ; curve direction detection

Ch1: MEMS gyroscope analogue output
Ch2: Left curve detection (vert. scale 5V/div)
Ch3: Right curve detection (vert.scale 5V/div)

11.2 Dynamical motion tests

11.2.1 Visual test
We checked by a visual observation the global correct behaviour of the small scale model car:
The system is inoperative in normal conditions of driving. And when driving fast enough in curve, to start a slipping, we observe against steering.

11.2.2 Reaction time measurement
We defined this reaction time as being the delta time between the initial instant "moment of the detection of a side slip" and the final instant "front wheels in against directing reaching their final angular position". For that purpose, we measure with an oscilloscope the delay time between a change in gyroscope output signal value and the final reached value of the PWM signal driving the servomotor. The movement of slip can be forced manually to facilitate measurement. The corresponding chronogram is given on figure 13.

Ch2: jerk detection (vert. scale 5V/div)
Ch3: output comparator slipping detection (vert. scale 5V/div);
Ch4: voltage image of wheels angular position (through potentiometer sensor in steering motor control block, vert. scale 5V/div)
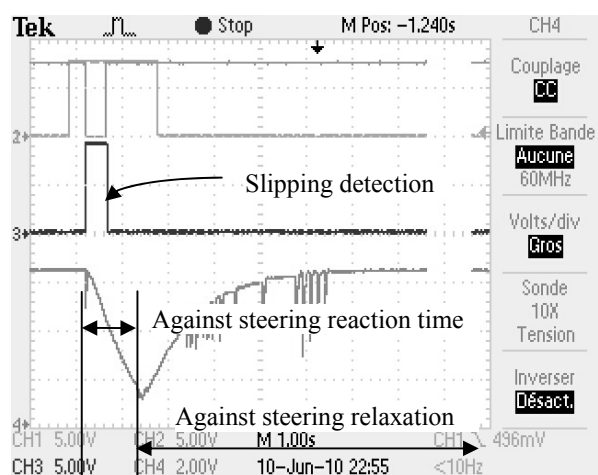
Figure 13: Response time.

The reaction time is representing the total reaction time due to electronic and steering motor time constants. Its value is around 500 ms (See paragraph § 8 for comments and discussions).

12. Discussion

12.1 Principe validation
The operation of "against steering" and its principle were validated. However, the reaction time of 500ms is too long to be effective during the turn of the vehicle. The reasons are identified and explained in the next paragraph 8.2.

12.2 Reaction time analysis
The intrinsic reaction time of our car is thus of approximately 500ms for total against steering. The response time is primarily limited by the mechanical reaction time of the servo traditional engine. This time would be correct and compatible for a vehicle scale 1:1. However, if our miniature vehicle is well respecting 1/14 scale for size, its weight is not divided by 14: our vehicle should be around 15 times heavier than it is. Thus, our vehicle has reaction similar to a "spinning top".

In scientific words, the kinetic moment $\Omega_m.J$ (where J is the inertial moment of the mobile) is too small. As J depends on the mass m of the mobile, one can add - if needed- a weight (ballast) at each extremity of the car to increase the moment of inertia. Thus, the rotation speed in slip will be slowed down. (As it was done with cement bags placed in the baggage cases, on the famous legendary rally car Renault R8 Gordini in the 1960').

A second possible improvement is to act on traction motor and steering wheels at the same time.

12.3 Improving the slipping detection
Jerk and multiplication process allows detecting the beginning of a back skid but not the end. Against steering is the automatically applied and progressively reduced till the end of the curve. Thus, it is a first help for the pilot. But, it is not a full reliable system. We would obtain information on peak value and slipping duration to improve the correction.

13. Conclusion
In this paper, we presented an original simplified electronic system for small model electrical car trajectory compensation. A first design was carried out, with interesting and concrete technical results. The complex embedded ESP system principle was partially "demystified". And all students involved in this project were satisfied with our "Learning by project" strategy.

As many technical improvements can be done on our prototype, this subject opens the way to many other projects for the next years.

References:
[1] « *ESP dispositif de contrôle de trajectoire* » http://www.willemin.net/Presse/Fonctionnement%20 ESP.pdf
[2] W. NUNINGER, W. PERRUQUETTI, JP. RICHARD « *Bilan et enjeux des modèles de frottements : tribologie et contrôle au service de la sécurité des transports.*" JEF'06, 5th European Conference on Braking, Lille, France (2006)
[3] Ch. Hyde *"Inertial Sensors Using Accelerometers & Gyro's*

for FIRST Robotics" Analog Devices power point presentation, January 2007

[4] J. Borenstein and L. Feng *"Gyrodometry: A New Method for Combining Data from Gyros and Odometry in Mobile Robots"* Proceedings of the 1996 IEEE International Conference on Robotics and Automation, Minneapolis, Apr. 22-28, 1996, pp. 423-428.

[5] T. L. Grigorie, N.Jula, C. Cepisca, C. Răcuciu, D. Răducanu *"Evaluation Method of the Sensors Errors in an Inertial Navigation System"* WSEAS TRANSACTIONS on CIRCUITS and SYSTEMS ISSN: 1109-2734 p.977 Issue 12, Volume 7, December 2008

[6] T. L. Grigorie, N.Jula, C. Cepisca, C. Răcuciu, D. Răducanu *"MEMS based Micro inertial measurement system"* WSEAS TRANSACTIONS on CIRCUITS and SYSTEMS ISSN: 1109-2734 p.691 Issue 5, Volume 5, May 2006

[7] Laurent Boutin, Mathieu Barreau « *réflexions sur l'énergétique des véhicules Routiers* » **A**ssociation de **S**auvetage **C**réatif du **S**avoir **A**érotechnique, juin 2008 http://inter.action.free.fr/

[8] C. VLOEBERGH, D.GRENIER, P.FISETTE, C.EUGENE, J-D LEGAT *"Intégration d'une compétition de robotique au sein du cursus de formation en mécatronique"* CETSIS EEA Nancy 25-27 October 2005

[9] Ph. DONDON- J.M MICOULEAU- G. LEROYER *" Initiation to GPS localisation and navigation using a small-scale model electric car: An illustration of "learning by project" for graduated students" "* WSEAS EDUTE 2009 24-26 october 2008 Genova (Italy)

[10] NikkoWebSite: http://nikkoevolution.fr/

[11] S.Allano, « *Petits moteurs électriques* » Techniques de l'ingénieur R1 940

[12] Mabuchi Web site : http://www.mabuchi-motor.co.jp

[13] N. Y. A. SHAMMAS, S. EIO, D. CHAMUND *"Semiconductor Devices and their use in Power Electronic Applications"* WSEAS POWER'07 21-23 Nov 2007 Venise (Italia)

[14] J.P Brossard « *Dynamique du véhicule, Modélisation des systèmes complexes* » ISBN: 2-88074-644-2 Presse polytechnique et universitaires romandes 2006

[15] P.Duysinx « *stabilité et comportement du virage en régime permanent* » cours université de Liège Belgique 2009

[16] Ch. Hyde *"Inertial Sensors Using Accelerometers & Gyro's for FIRST Robotics"* Analog Devices power point presentation, January 2007

[17] Invensense IDG 650 data sheet Website: www.invensense.com